Simulations of Computer, Telecommunications, Control and Social Systems

Моделирование вычислительных, телекоммуникационных, управляющих и социально-экономических систем

FINITE ELEMENT SIMULATION OF SAW DELAY LINE OPERATING WITH THE USE OF THIRD HARMONIC FREQUENCY

A.S. Koigerov[1] ✉, O.L. Balysheva[2]

[1] St. Petersburg Electrotechnical University "LETI",
St. Petersburg, Russian Federation;
[2] Saint-Petersburg State University of Aerospace Instrumentation,
St. Petersburg, Russian Federation

✉ a.koigerov@rambler.ru

Abstract. A numerical practical approach for a simulation of surface acoustic wave delay line is proposed. The principle of operation of transducers with split electrodes at frequency harmonics is shown. Practical recommendations and calculation algorithm in COMSOL Multiphysics are considered. Admittance parameters were calculated from simulations of delay line employing COMSOL software. Finally, obtained Y-parameters were converted into a full set of S-parameters. The numerical approach makes it possible to accurately model the SAW device using the universal finite element method with automatic inclusion of second-order effects in the device. To demonstrate the finite element method, the frequency response for 1.5 GHz SAW delay line with a relative bandwidth of 7.46 % on 128° YX-cut $LiNbO_3$ are calculated. Input interdigital transducer operates at main frequency, output transducer operates at the third harmonic frequency. The simulation results are in good agreement with the experimental data.

Keywords: surface acoustic waves, SAW, delay line, numerical approach, finite element method, lithium niobate, piezoelectric substrate

КОНЕЧНО-ЭЛЕМЕНТНОЕ МОДЕЛИРОВАНИЕ ЛИНИИ ЗАДЕРЖКИ НА ПАВ, РАБОТАЮЩЕЙ С ИСПОЛЬЗОВАНИЕМ ТРЕТЬЕЙ ЧАСТОТНОЙ ГАРМОНИКИ

А.С. Койгеров[1] ✉, О.Л. Балышева[2]

[1] Санкт-Петербургский государственный электротехнический университет «ЛЭТИ» им. В.И. Ульянова (Ленина), Санкт-Петербург, Российская Федерация;

[2] Санкт-Петербургский государственный университет аэрокосмического приборостроения, Санкт-Петербург, Российская Федерация

✉ a.koigerov@rambler.ru

Аннотация. Рассмотрен численный практический подход моделирования линии задержки на поверхностных акустических волнах. Показан принцип работы преобразователей с расщепленными электродами на гармониках. Приведены практические рекомендации и алгоритм расчета для моделирования в пакете COMSOL Multiphysics. Характеристики адмиттанса рассчитаны из моделирования линии задержки на поверхностных акустических волнах с помощью метода конечных элементов в COMSOL. В результате расчета полученные Y-параметры преобразованы к полному набору S-параметров. Рассматриваемый численный подход на основе метода конечных элементов дает возможность рассчитать линию задержки на поверхностных акустических волнах с учетом «вторичных эффектов». Представлены результаты расчета амплитудно-частотной характеристики линии задержки с относительной полосой пропускания 7,46 % для частоты 1,5 ГГц на подложке 128° YX-среза ниобата лития. Входной встречно-штыревой преобразователь работает на основной гармонике, выходной преобразователь — на третьей гармонике. Результаты моделирования хорошо согласуются с экспериментальными данными.

Ключевые слова: поверхностные акустические волны, линия задержки на ПАВ, численный подход, метод конечных элементов, ниобат лития, пьезоэлектрическая подложка

Introduction

Currently, surface acoustic wave (SAW) devices (filters, delay lines (DL), resonators, etc.) are used in various radio engineering systems. So, SAW filters [1, 2] are key elements of modern communication systems and radio equipment. SAW tag and wireless sensors [3, 4] solve the problems of identifying and measuring the parameters of the ambient environment for various applications from individual autonomous sensors to industrial automation systems.

In recent years, there has been growing interest in the use of SAW devices at gigahertz frequencies. It is known that the interdigital transducer (IDT) can operate not only at fundamental, but at harmonic frequencies [5–8]. Moreover, the intensity of their excitation depends on the metallization coefficient (the ratio of the electrode width a to the pitch of the IDT electrodes p: a/p), the thickness of the metallization, the shape of the electrode and the type of transducer. An analysis of higher-order harmonics from the metallization ratio for Rayleigh waves is investigated in [5]. Propagation and resonant properties of harmonics of leaky SAW are presented in [9]. The characteristics of non-linear harmonic bulk

acoustic wave (BAW) mode generation in SAW devices have been learned and presented in [10, 11]. Experimental and theoretical studies of harmonic operation for various classes of SAW devices are presented in [12−16], for example, two-port resonators [12], filters [13], tags [14], sensors [15], devices with temperature compensation SAW [16].

This approach based on higher-order harmonics makes it possible to manufacture SAW devices operating at frequencies above 2.5 GHz without the use of submicron lithography methods. But it is worth noting a number of disadvantages inherent in harmonics:

1) high insertion loss with increasing frequency;
2) presence of a spectrum of bulk acoustic waves that are excited in the same frequency range;
3) presence of unwanted harmonics that can be excited simultaneously.

Generally, designers and users would like the SAW devices to operate on one selected harmonic while suppressing other unwanted harmonics.

Designing SAW devices is a complicated technical problem, because there are complex acoustic relationships between the element of the topology, the resonant behavior of the acoustic processes, the high sensitivity of the electrical parameters to the geometry of the elements, and also all this depends on the parameters of the acoustic waves and the piezoelectric material. To calculate LC-filters and filters based on LC-prototypes, there is specialized software, such as AWR Microwave Office, HFSS, ADS, CST Studio Suite. Methods for synthesizing LC-filters are fairly well known. There are no unified approaches and programs for calculating SAW devices; each developer uses different modeling approaches and their own software. The only more or less unified approach can be called the approach based on the finite element method (FEM). In addition, the problem of using frequency harmonics deserves special attention. Since the SAW devices mainly operate on the fundamental harmonic, the technological limit of operation is limited to a value of the order of 2.5...3 GHz. The use of frequency harmonics potentially allows operation in a higher frequency range.

Today the most popular software for numerical modeling of SAW/BAW devices are COMSOL and ANSYS. These software products have proven to be a powerful tool for analyzing wave acoustic processes in piezoelectric crystals and for SAW/BAW devices calculations [17−21].

The aim of the work is to show the state of the art and the main features of the calculation of the SAW DL using the third harmonic based on the finite element method in the COMSOL. As a sample, on the basis of which the results of calculation and experiment will be compared, the design of a DL on a substrate of a 128° YX-cut of lithium niobate was chosen.

SAW delay line model

Fig. 1*a* shows a typical SAW delay line (DL) topology, which consists of an input and output IDT located on a piezoelectric substrate. The DL is represented as a two-port device in the system of Y-parameters (Fig. 1*b*).
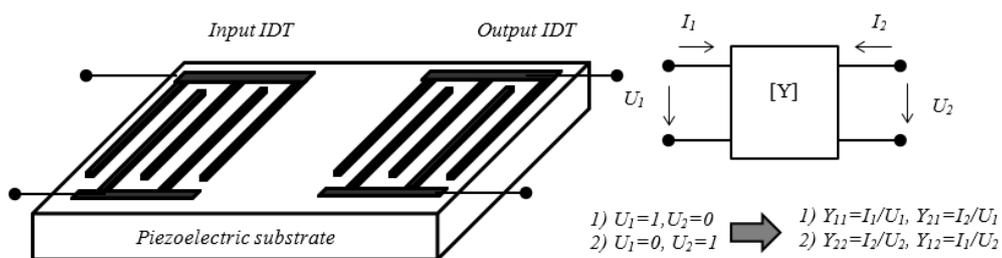

Fig. 1. SAW delay line: *a* − typical topology; *b* − the device in the system of Y-parameters and the principle of switching electrical ports for finding Y-parameters
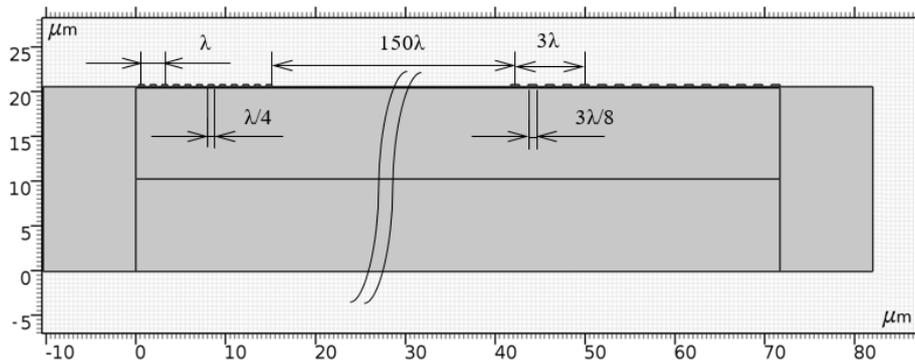
Fig. 2. Geometry in COMSOL

To model this device in the COMSOL, it is necessary to accurately outline the geometry of the SAW DL. Fig. 2 shows the DL geometry and its main parameters. A 128° YX-cut of lithium niobate was chosen as the piezoelectric substrate. The operating wavelength is $\lambda = 2.6$ μm, which corresponds to a frequency of about 1.5 GHz. The considered delay is about 100 ns, so the distance between the IDTs is about 150 λ.

The principle of operation of the device at frequency harmonics

Fig. 3 shows the results of calculating admittance parameters by FEM for various types of transducers. At Fig. 3*a* one you observe the admittance of the split transducer with electrodes $\lambda/8$ ($\lambda = 2.6$ μm) with the number of periods $N = 6$. It is clearly seen that, in addition to the fundamental mode at a frequency of 1.5 GHz, there is a third harmonic at a frequency of about 4.5 GHz. Besides, you can see that, in addition to the 3rd harmonic, there is a fairly strong BAW radiation. Fig. 3*b* shows the admittance parameters of the transducer with electrodes $\lambda/4$ and the transducer with split electrodes $3\lambda/8$. It can be seen that the fundamental mode for the IDT with $\lambda/4$ corresponds to a frequency of 1.5 GHz, while for the IDT with split electrodes, the fundamental mode is now at a frequency of 0.5 GHz, and the 3rd harmonic is located at a frequency of 1.5 GHz. Using this combination of IDTs as the input and output IDTs for the SAW DL, we calculate the complete set of Y-parameters for the DL as a whole.
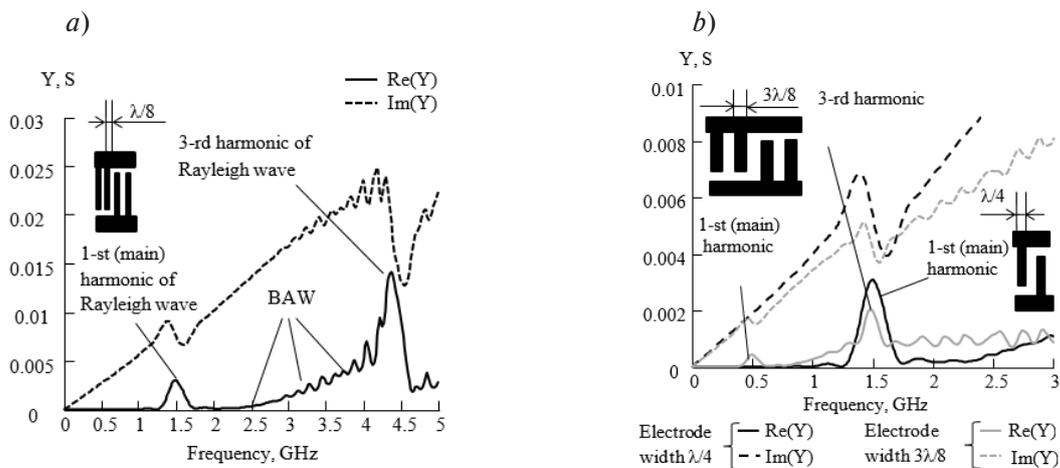

Fig. 3. Principle of operation of the IDT at harmonics: *a* − fundamental and 3rd harmonic of the IDT with split electrodes (width of electrodes $\lambda/8$); *b* − fundamental and 3rd harmonic excitation for IDT with split electrodes (electrode width $3\lambda/8$) and only fundamental for IDT with $\lambda/4$ electrodes

Calculation algorithm in COMSOL

In contrast to the one-dimensional consideration of the problem in such analytical and phenomenological approaches as the model "coupling of modes" (COM) [22] and the equivalent circuit model [23], finite element modeling allows one to obtain the necessary parameters and characteristics in three dimensions, including exactly obtain information on the scattering of the wave into the depth of the substrate. Moreover, the developer receives information about all excited acoustic modes in a specific topology and material, in contrast to COM and equivalent circuit model, where the classical approach involves the calculation of the main acoustic mode. In essence, such simulation will be the most accurate in terms of describing all acoustic processes. By optimizing and simplifying the model, we consider several conditions:

1. The transducer should not have apodization (amplitude weighing).

2. The wave propagating from the transducer has a flat front. This assumption is possible with an IDT aperture of more than 15 wavelengths; in this case, the waveguide effect can be neglected [24].

3. If distance between adjacent blocks (IDT) is insignificant, diffraction can also be ignored [25].

4. Solution obtained in a small area of the aperture will be extended to an entire transducer with an accuracy up to an aperture factor.

5. We neglect the influence of bus bars.

It is clear that these conditions significantly narrow the range of analyzed topologies of SAW devices, but at the same time they are suitable for the class of SAW DL. The ultimate goal of the calculation is to find a set of parameters that completely describe the device. Such parameters can be Z-, Y- or S-parameters of a device. Using the FEM, it is convenient to calculate a set of Y-parameters, and using already known formulas, go to a set of S-parameters [26]. The DL is represented as a two-port device in the system of Y-parameters (Fig. 1b). Current I_1 and voltage U_1 act on the input electrical port 1 of the DL, current I_2 and voltage U_2 are formed on the output electrical port 2. Thus, it is necessary to find the dependencies in the frequency domain of a set of Y-parameters (Y_{11}, Y_{12}, Y_{21}, Y_{22}). Since SAW DL belongs to the class of linear passive circuits, it is necessary to find at least three independent components, because ($Y_{12} = Y_{21}$).

The main purpose of the simulation is to calculate the SAW DL with characteristics that meet certain technical requirements. The main steps of the calculation algorithm using the COMSOL Multiphysics simulation layout are displayed in a block diagram (Fig. 4), which breaks one large task into several stages or steps that succinctly characterize the described approach.

Step 1. Preliminary preparation of the model in COMSOL. Choice of model dimension and physical partition or interface. It is necessary to choose the right one from the available set of physical interfaces that allow you to simulate the necessary physical phenomena quickly; in our case, this is the piezoelectric effect. Select "Piezoelectric Devices".

Step 2. Analysis of the technical requirements for the device. The analysis allows you to set the main restrictions on the dimensions of the structure and restrictions on materials, taking into account temperature deviations.

Step 3. Selecting the device geometry. At this stage, based on the formulated technical requirements, it is necessary to determine the type of device geometry, the profile of the electrodes, and the thickness and metallization coefficient of the electrodes. In some cases, it is also necessary to determine the material of the underlayer and its thickness.

Step 4. Drawing the geometry (topology) of the device.

Step 5. Choice of electrode materials. Selection from the library or input of constants for metal electrodes: Young's modulus, Poisson's ratio, density.

Step 6. Choice of substrate materials. To describe piezoelectric substrates, we need matrices of elastic coefficients, piezoelectric constants, dielectric constants, and density. They can be taken either from the available library, or manually entered from well-known sources, for example [27]. The required Euler angles are given in [25].
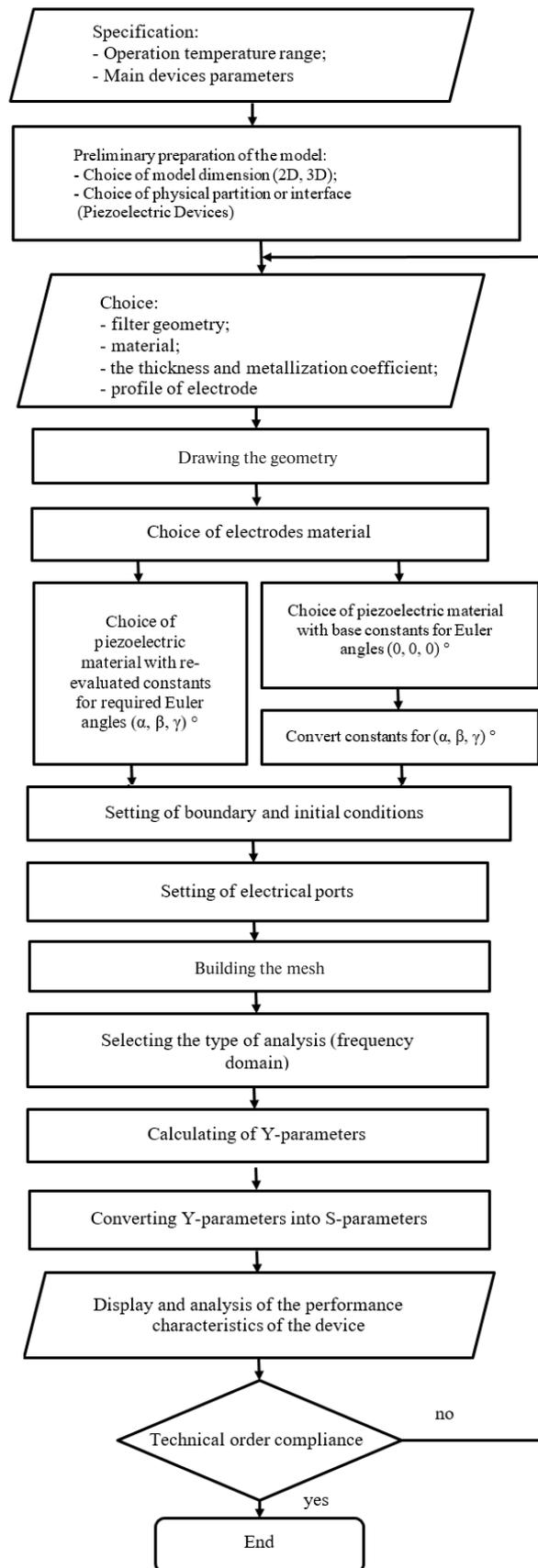
Specification:
- Operation temperature range;
- Main devices parameters

Preliminary preparation of the model:
- Choice of model dimension (2D, 3D);
- Choice of physical partition or interface
 (Piezoelectric Devices)

Choice:
- filter geometry;
- material;
- the thickness and metallization coefficient;
- profile of electrode

Drawing the geometry

Choice of electrodes material

Choice of
piezoelectric
material with re-
evaluated constants
for required Euler
angles (α, β, γ) °

Choice of piezoelectric material
with base constants for Euler
angles $(0, 0, 0)$ °

Convert constants for (α, β, γ) °

Setting of boundary and initial conditions

Setting of electrical ports

Building the mesh

Selecting the type of analysis (frequency
domain)

Calculating of Y-parameters

Converting Y-parameters into S-parameters

Display and analysis of the performance
characteristics of the device

Technical order compliance

no

yes

End

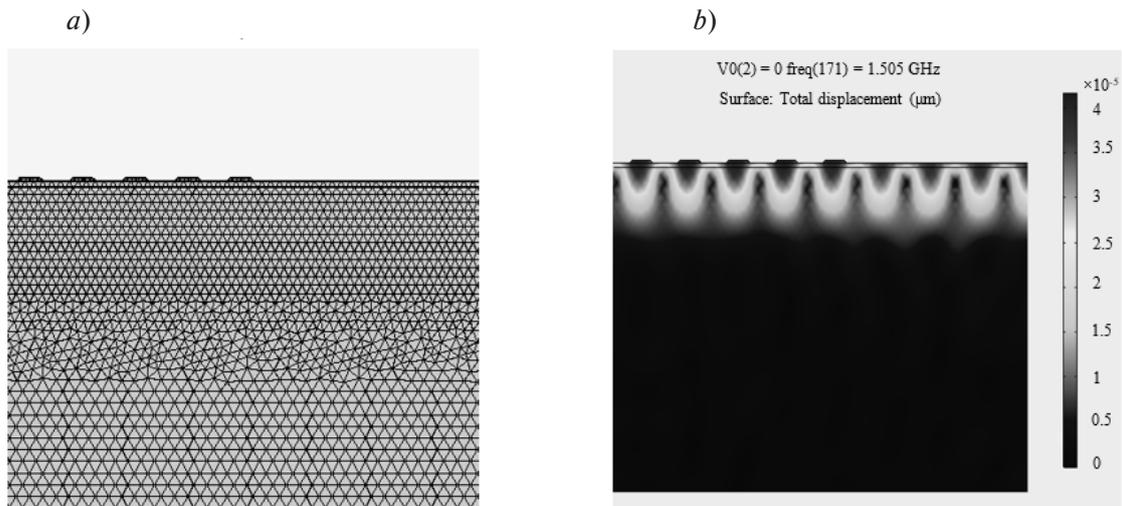Fig. 4. Calculation algorithm in COMSOL

a)

b)

Fig. 5. Example of a display for a fragment of the delay line geometry:
a — grid; *b* — mechanical displacement

Step 7. Setting of boundary conditions and initial conditions. It is necessary to specify the conditions of the free surface from above and the periodic boundary conditions for the aperture. Boundary conditions are divided into mechanical and electrical.

Step 8. Setting up electrical ports. To calculate Y_{11}, Y_{21}, you must set the state of the electrical ports $U_1 = 1$, $U_2 = 0$, to calculate Y_{22}, $Y_{12} - U_2 = 1$, $U_1 = 0$.

Step 9. Building the mesh. It is necessary to form a grid, that is to break the model into finite elements. In this paper, we will consider the ratio by the size of finite elements $m = \lambda/12$ (Fig. 5*a*), where m is the size of the side of the finite element, λ is the wavelength. The division of the model into areas is phenomenological in nature, therefore, depends on the available skills. Poor partitioning can lead to inaccurate results. The region discretization procedure consists of specifying the number, size, and shape of subregions, which are used to construct a discrete model of a real object. There is currently no unified method for partitioning into finite elements, and the most effective partitioning method is the experience and understanding of the physics of the described object.

Step 10. Selecting the type of analysis. In this case, we are interested in analysis in the frequency domain. Let us move on to choosing the frequency analysis range and the number of frequency points.

Step 11. Calculation of Y-parameters. As a result of the calculation, we have a large set of solutions in terms of the number of degrees of freedom (DOF) for each parameter (3 components of mechanical displacement (Fig. 5*b*)) and potential taking into account the degree of finite element discretization. Internal means, you can go to the device parameters of interest, in our case it is the admittance, for example, these are the real and imaginary parts of the admittance. Ultimately, it is necessary to obtain a complete set of Y-parameters.

Step 12. "Post-processing". Transition from a set of Y-parameters to a set of S-parameters. A two-port device is conveniently described not as a set of Y-parameters, but as elements of a scattering matrix or S-parameters, since the performance characteristics of the device (for example, frequency response) are described by similar characteristics. The physical meaning of S_{11} is the reflection coefficient at the input, S_{21} is the complex transfer coefficient. Most often, S-parameters are determined in a path with a characteristic impedance $Z_0 = 50$ Ohm.

Step 13. Display and analysis of the performance characteristics of the device (frequency response, group delay, etc.) for compliance with technical requirements. The results of the calculated frequency response are shown in Fig. 6*a*.
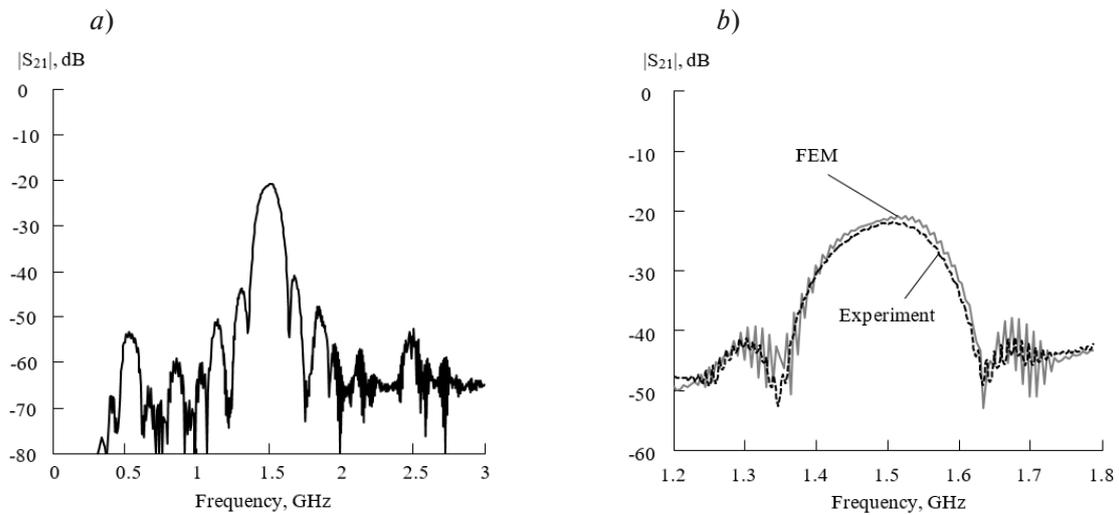
a)

b)

Fig. 6. Frequency response: *a* − calculated without "parasitic" LC-elements;
b − calculated with "parasitic" LC-elements and experimental

Experiment

The manufactured SAW DL consisted of two transducers. The input is a bidirectional transducer with $\lambda/4$ electrodes, operating on the fundamental mode, the output is a split-electrode transducer with an electrode width of $3\lambda/8$, operating at the 3rd harmonic. The delay line operates at 1.5 GHz. The device is made on a 128° YX-cut lithium niobate. The input IDT consists of 6 pairs of electrodes. The output IDT − 4. The absolute value of the metallization thickness is $H_m = 75$ nm, the relative value is $H_m/\lambda = 2.9$ %. Fig. 7 shows a circuit with "parasitic" LC elements, the inclusion of which made it possible to compare the theoretical and measured frequency responses shown in Fig. 6. The DL has a center frequency of 1.5 GHz and a bandwidth of 112 MHz or 7.46 % (for attenuation level of −3 dB). Insertion loss was −22.2 dB. The results showed good agreement between numerical simulation and experiment.

Discussion

The practice of using the COMSOL for modeling SAW devices allows us to draw some conclusions. The considered approach based on numerical analysis of FEM in the COMSOL Multiphysical modeling may be required to design SAW devices, since it provides greater accuracy of calculations. The main disadvantage is accounting for a variety of parameters in 3D modeling of real full-aperture devices leads to a dramatic increase in requirements for computing resources and an increase in analysis time. Therefore,
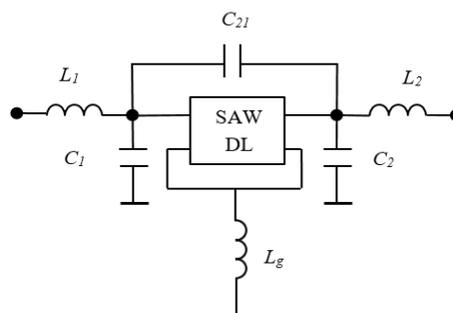

Fig. 7. Scheme with "parasitic" LC elements

this approach is more suitable for analyzing devices at the final stage of development, where we can replace a real experiment with high-quality multiphysical modeling. In addition, there are combined approaches that allow you to get results much faster and are used, as a rule, for preliminary evaluation of characteristics at the synthesis stage and topology adjustments. A feature of calculations with combined approaches is the need to find the model parameters beforehand. Within the framework of the combined approach, the necessary parameters can be extracted from simple test cells [28] using FEM. This combined approach includes the advantages of a fast analytical model with the accuracy obtained when calculating the entire device only with FEM.

Some of the complexities and disadvantages inherent in the software in full 3D mode are compensated by high calculation accuracy, as well as the ability to solve particular problems, for example, in truncated models.

Conclusion

The paper showed the state of the art and the main features of the SAW DL simulation using the third harmonic based on the FEM in the COMSOL Multiphysics. The calculated values of the set of Y-parameters made it possible to determine the S-parameters, for example, the frequency response. The results obtained show a good agreement between the simulation and experimental results.

The difference in responses in the passband does not exceed 0.7 dB, in the stopband − 4 dB. The differences of the calculated and experimental results can be due to more complex circuit the parasitic inductances and capacitances of the connecting wires, contact buses, and housing, and also the presence of wave diffraction in the real DL. The DL has a center frequency of 1.5 GHz and a bandwidth of 112 MHz or 7.46 %, insertion loss −22.2 dB, stopband attenuation −20 dB. The use of the COMSOL Multiphysics makes it possible to accurately evaluate the characteristics of the devices being developed without making a physical prototype.

Acknowledgment

REFERENCES

1. **Bagdasaryan A.S., Gulyaev Yu.V., Dobershtein S.A., Sinitsina T.V.** Low-loss SAW filters − one of major competitive advantages of SAW technology. *Radio Communication Technology*, 2019, Iss. 3 (42), Pp. 86−98. (rus). DOI: 10.33286/2075-8693-2019-42-86-98

2. **Doberstein S.A.** Balanced low-loss narrowband double mode saw filters with improved selectivity. *Radio Communication Technology*, 2019, Iss. 4 (43), Pp. 79−85. (rus). DOI: 10.33286/2075-8693-2019-43-79-85

3. **Ancev I.G., Bogoslovsky S.V., Sapognikov G.A., Zhgoon S.A., Shvetsov A.S.** Surface acoustic wave temperature sensor. *Sensors and Systems*, 2018, no. 1 (221), Pp. 40−48. (rus)

4. **Reut V.R., Koigerov A.S., Andreychev S.S., Dorokhov S.P., Salov A.S.** The new design of SAW ID tags on base of multistrip coupler. *Nano- i Mikrosistemnaya Tekhnika*, 2019, Vol. 21, no. 10, Pp. 579—593. DOI: 10.17587/nmst.21.579-593

5. **Campbell C.K.** Obtaining the fundamental and harmonic radiation conductances of a reflective SAW interdigital transducer. *Proceedings of the IEEE Ultrasonics Symposium*, 1998, Vol. 1, Pp. 169−173. DOI: 10.1109/ULTSYM.1998.762124

6. **Campbell C.K., Edmonson P.J.** Conductance measurements on a leaky SAW harmonic one-port resonator. *IEEE Transactions on Ultrasonics, Ferroelectrics, and Frequency Control*, Jan. 2000, Vol. 47, no. 1, Pp. 111−116. DOI: 10.1109/58.818753

7. **Morgan D.P.** Reflective array modeling for reflective and directional SAW transducers. *IEEE Transactions on Ultrasonics, Ferroelectrics, and Frequency Control*, Jan. 1998, Vol. 45, no. 1, Pp. 152−157. DOI: 10.1109/58.646919

8. **Zhai F., Zhang D.** The dual harmonic interdigital transducers (DHIDT). *Proceedings of International Frequency Control Symposium*, 1997, Pp. 845−851. DOI: 10.1109/FREQ.1997.639201

9. **Asakawa S., Suzuki M., Kakio S., Tezuka A., Mizuno J.** Resonance properties of leaky SAW harmonics on bonded dissimilar-material structures. *Proceedings of the IEEE International Ultrasonics Symposium* (*IUS*), 2020, Pp. 1−3. DOI: 10.1109/IUS46767.2020.9251535

10. **Pang X., Yong Y.** Characteristics of BAW modes harmonically generated (f-2f-3f) in LiNO3 SAW devices. *2019 Joint Conference of the IEEE International Frequency Control Symposium and European Frequency and Time Forum* (*EFTF/IFC*), 2019, Pp. 1−2, DOI: 10.1109/FCS.2019.8855990

11. **Pang X., Yong Y.** Simulation of nonlinear resonance, amplitude−frequency, and harmonic generation effects in SAW and BAW devices. *IEEE Transactions on Ultrasonics, Ferroelectrics, and Frequency Control*, Feb. 2020, Vol. 67, no. 2, Pp. 422−430. DOI: 10.1109/TUFFC.2019.2945522

12. **Sato T., Otsuka S., Okajima H., Motegi R.** Experimental investigation on the operation of SAW devices at harmonic frequencies with stepped-finger interdigital transducer. *Proceedings of the IEEE Ultrasonics Symposium*, 1996, Vol. 1, Pp. 267−270. DOI: 10.1109/ULTSYM.1996.583971

13. **Huegli R.** GHz filters with third harmonic unidirectional transducers. *IEEE Symposium on Ultrasonics*, 1990, Vol. 1, Pp. 165−168. DOI: 10.1109/ULTSYM.1990.171345

14. **Chen Y., Wu T., Chang K.** A COM analysis of SAW tags operating at harmonic frequencies. *Proceedings of the IEEE Ultrasonics Symposium*, 2007, Pp. 2347−2350. DOI: 10.1109/ULTSYM.2007.590

15. **Hikita M., Kato Y., Matsuda J., Watanabe T., Nakano A.** Self-temperature-compensation characteristics at 1st- and 3rd-harmonic frequencies for SAW gas sensor used in sensor network. *IEEE International Ultrasonics Symposium*, 2009, Pp. 2496−2499. DOI: 10.1109/ULTSYM.2009.5441984

16. **Chauhan V., et al.** A nonlinear FEM model to calculate third-order harmonic and intermodulation in TC-SAW devices. *IEEE International Ultrasonics Symposium* (*IUS*), 2018, Pp. 1−9. DOI: 10.1109/ULTSYM.2018.8580153

17. **Koigerov A.S., Balysheva O.L.** Numerical approach for extraction COM surface acoustic wave parameters from periodic structures analysis. *Wave Electronics and its Application in Information and Telecommunication Systems* (*WECONF*), 2021, Pp. 1−6. DOI: 10.1109/WECONF51603.2021.9470638

18. **Dvoesherstov M.Yu., Cherednic V.I., Bosov S.I., Orlov I.Ya., Rudenko O.V.** Numerical and experimental analysis of the parameters of an electroacoustic thin-film microwave resonator. *Acoustic Physics*, 2013, Vol. 59, no. 5, Pp. 513−520. DOI: 10.7868/S0320791913050079

19. **Zhang Y., Jin J., Li H., Hu H.** A novel method to extract COM parameters for SAW based on FEM. *13th Symposium on Piezoelectricity, Acoustic Waves and Device Applications* (*SPAWDA*), 2019, Pp. 1−5. DOI: 10.1109/SPAWDA.2019.8681838

20. **Papirovskiy A.A., Lukin A.V., Popov I.A.** O metodakh modelirovaniya volnovykh protsessov v p'yezoakusticheskikh preobrazovatelyakh. *Nedely Nauki SPbPU. Materialy nauchnoy konferentsii s mezhdunarodnym uchastiem*, 2018, Pp. 314−316. (rus)

21. **Osetrov A.V., Myshinsky E.L.** Anisotropy accounting inhjmogeneous modes of surface acoustic waves. *Noise Theory and Practice*, 2018, Vol. 4, no. 4 (14), Pp. 28−34. (rus)

22. **Dmitriev V.F.** Modified equations of coupled surface acoustic waves. *Journal of Communications Technology and Electronics*, 2009, Vol. 54, no. 9, Pp. 1134−1143. DOI: 10.1134/S1064226909090137

23. **Gonzalez-Rodriguez M., Collado C., Mateu J., Gonzalez-Arbesu J.M., Huebner S., Aigner R.** Fast simulation method of distributed nonlinearities in surface acoustic wave resonators. *IEEE International Ultrasonics Symposium* (*IUS*), 2020, Pp. 1−4. DOI: 10.1109/IUS46767.2020.9251549

24. **Sveshnikov B.V., Bagdasaryan A.S.** The main principles of formation of the transverse modes in the multilayered waveguides of surface acoustic waves. *Radiophys Quantum*, 2016, El 59, Pp. 97−110. DOI: 10.1007/s11141-016-9679-5

25. **Morgan D.** *Surface acoustic wave filters with applications to electronic communications and signal processing.* Academic Press, 2010. 448 p.

26. **Hong J., Lancaster M.J.** *Microstrip filters for RF/microwave applications.* John Wiley & Sons. Inc., 2001. 457 p.

27. **Kovacs G., et al.** Improved material constants for LiNbO3/ and LiTaO3. *IEEE Symposium on Ultrasonics*, 1990, Vol. 1, Pp. 435−438. DOI: 10.1109/ULTSYM.1990.171403

28. **Koigerov A.S., Balysheva O.L.** Numerical analysis of parameters of pseudosurface acoustic wavesin lithium niobate and tantalate crystals. *Journal of Communications Technology and Electronics*, 2021, Vol. 66, No. 12, Pp. 1388−1395.

INFORMATION ABOUT AUTHORS / СВЕДЕНИЯ ОБ АВТОРАХ

Aleksey S. Koigerov
Койгеров Алексей Сергеевич
E-mail: a.koigerov@rambler.ru

Olga L. Balysheva
Балышева Ольга Леонидовна
E-mail: balysheva@mail.ru